Iron in silicon: Interactions with radiation defects, carbon, and oxygen

S. K. Estreicher,* M. Sanati, and N. Gonzalez Szwacki
Physics Department, Texas Tech University, Lubbock, Texas 79409-1051, USA
(Received 21 December 2007; revised manuscript received 29 January 2008; published 26 March 2008)

First-principles theory is used to calculate the interactions between interstitial iron or the iron-boron pair and a vacancy, between interstitial iron and a divacancy, oxygen-vacancy pair, self-interstitial, and interstitial carbon, as well as substitutional carbon, interstitial oxygen, and the oxygen dimer in silicon. The structures, charge and spin states, binding energies, and, in some cases, vibrational spectra are predicted. The gap levels are estimated using the marker method. The strongest interactions involve vacancies, result in the formation of pairs of metastable defects, and profoundly change the electrical activity of the component species. Iron also traps at self-interstitial-type defects, but not at interstitial oxygen or substitutional carbon. Several observed but incompletely characterized defects are identified and trends in the behavior of Fe in Si are discussed.

DOI: 10.1103/PhysRevB.77.125214 PACS number(s): 71.55.Eq, 61.72.Bb

I. INTRODUCTION

Iron is one of the most undesirable yet unavoidable transition metal impurities in integrated circuit as well as photovoltaic Si. Many iron-related defects are recombination centers and reduce minority carrier lifetimes, while Fe clusters and precipitates at Si/SiO_x interfaces degrade the gate oxide integrity. The numerous sources of iron contamination as well as the experimental and theoretical research on Fe-related defect centers have been reviewed.[1,2]

In the first paper of this series,[3] we have reported our predictions about interstitial iron (Fe_i), iron-acceptor pairs $\{Fe_iA_s\}$ (where $A=B,Al,Ga,In,Tl$), iron interactions with shallow substitutional donors (P and As), as well as the interactions of interstitial hydrogen with Fe_i and the $\{Fe_iB_s\}$ pair. This paper also contains the details of the methodology we use as well as comparisons between calculated and measured donor and acceptor levels. The present study uses the same theoretical approach but focuses on less well documented interactions.

We report here studies of iron interacting with radiation damage. Specifically, we investigate the complexes resulting from the interactions between a preexisting vacancy (V) and Fe_i and the $\{Fe_iB_s\}$ pair, the interactions of Fe_i with the divacancy (V_2), the A center[4,5] ($\{OV\}$ pair), the self-interstitial (Si_i), and interstitial carbon[6,7] (C_i). For completeness, we consider the interactions between Fe_i and substitutional carbon (C_s) and interstitial oxygen (O_i), which are the most abundant impurities in as-grown float-zone (FZ) and Czochralski (Cz) silicon, respectively. We also include the interstitial oxygen dimer $\{O_iO_i\}$.

Section II contains a review of the experimental situation. Section III summarizes the level of theory. The details are described in Ref. 3 and are not repeated here. Sections IV and V deal with the interactions of V and Fe_i and the $\{Fe_iB_s\}$ pair, respectively. Sections VI–IX discuss the interactions of Fe_i with V_2, $\{OV\}$, Si_i, and C_i, respectively. Section X completes the picture by examining the possibility of pairing between Fe_i and C_s, O_i, and the $\{O_iO_i\}$ pair. The results are discussed in Sec. XI.

II. EXPERIMENTAL INFORMATION

The most common iron-related defects[2,3] in Si are isolated Fe_i and, in p-type Si, the iron-acceptor $\{Fe_iA_s\}$ pair. The former is at the tetrahedral interstitial (T) site. In p-type Si, it has charge +1 with spin 3/2 ($^{3/2}Fe_i^+$). In intrinsic and n-type Si, it has charge 0 with spin 1 ($^1Fe_i^0$). The latter has Fe_i trapped very near one of the nearest or one of the second-nearest T sites to the substitutional shallow acceptor A_s (A is B, Al, Ga, In, or Tl) in a trigonal or orthorhombic configuration, respectively.

The $\{Fe_iA_s\}$ pair is weakly bound and dissociates at moderate temperatures. In the case of $\{Fe_iB_s\}$, a 30 s annealing at 180 °C fully dissociates the pairs. The process is reversible. At room temperature, Fe_i^+ diffuses toward A_s^- and the pair forms again. Choi *et al.*[8] reported a substantial increase in the concentration of $\{Fe_iB_s\}$ pairs when the sample is left at room temperature for several days following the 180 °C annealing. They suggested that some electrically inactive form of Fe was present in their sample.

The situation is more complicated in irradiated or implanted samples, where Fe_i interacts with preexisting vacancies and self-interstitials. Muller *et al.*[9] diffused Fe at 1200 °C for 16 h into large high-resistivity FZ-Si samples and performed electron paramagnetic resonance (EPR) experiments at low temperatures. Then, the samples were irradiated at room temperature with 1.8 MeV electrons, briefly annealed, and EPR measurements were performed again.

Two EPR centers observed before irradiation are believed not to involve native defects. NL22, a trigonal center with spin 4 and four Fe atoms, was proposed to consist of four neutral interstitial Fe atoms. NL22 anneals out around 160 °C. NL24, first assumed to be irradiation-related but later seen[10] as a quenched-in defect, has monoclinic I symmetry, two equivalent Fe atoms, and probably spin 5/2 with g close to 2 (a fit to a spin 1/2 Hamiltonian is also possible but leads to unusual g values). NL24 anneals out at 60 °C and was proposed to be a $\{Fe_iFe_i\}^+$ pair.

Numerous EPR centers appear following electron irradiation, but only five of them could be resolved.[9] NL19 is trigonal, contains one Fe atom, has spin 3/2, and anneals out at 160 °C. It was proposed to be a trigonal iron-vacancy pair, $\{Fe_iV\}^+$. NL20 is also trigonal, contains two Fe atoms, has spin 1/2 or 5/2, and anneals out at 160 °C. A trigonal $\{Fe_iVFe_i\}^+$ complex was proposed. NL21 is monoclinic I, contains two Fe atoms, has spin 1/2 or 5/2, and anneals out

at 250 °C. The model was a $\{Fe_iV_2Fe_i\}^+$ complex. NL23 is triclinic with spin 1/2 and anneals out at 100 °C. The number of Fe atoms involved was not resolved, and no model has been proposed for it. Finally, NL25 is rhombic II, contains two Fe atoms, has spin 5/2, and anneals out at 150 °C. The model was also a $\{Fe_iVFe_i\}^+$ complex.

Mchedlidze and Suezawa[11–13] performed a similar set of experiments, but with more energetic (3 MeV) e^- irradiation. They reported a trigonal spin 3/2 defect containing Fe which was described first as one defect, and then as two distinct defects (TU1 and TU2).[11] It was also referred to as the NL19 iron-vacancy $\{Fe_iV\}$ center discussed above. Although the spin, symmetry, and involvement of a single Fe atoms match, the g tensors of NL19 and the new defect(s) are not quite the same, which was first suspected to be due to a slight misalignment of the samples.[14] The defect was later described using the same spin Hamiltonian parameters as NL19.[12] However, the new defect anneals out[13] near 500 °C, which is much higher than the temperature at which NL19 disappears (160 °C), and implies a defect more stable than the divacancy or the A center. Another trigonal center with spin 1 was described as a different configuration of the same center. Since a change of spin from 3/2 to 1 implies that the number of odd electrons changes by 1, it would have to be a different charge state. Yet, the relative intensities of the spin 3/2 and spin 1 defects are independent of the doping, irradiation dose, or illumination.[11]

Another trigonal center was reported in the same study.[13] It contains two iron atoms and was interpreted as the NL20 ($\{Fe_iVFe_i\}^+$) defect. However, it too anneals out at higher temperatures (300–350 °C) than its NL counterpart (160 °C). Photo-EPR data[13,15] show that the defect assigned to the $\{Fe_iV\}$ center has a hole trap at $E_v+0.50$ eV, while the defect assigned to the $\{Fe_iVFe_i\}$ center has a trap at $E_v+0.53$ eV.

Experimental information about Fe interactions with native defects has also been provided by Mössbauer spectroscopy.[16–19] In these experiments, ^{57}Mn is implanted and decays into ^{57}Fe with a half-life $\tau_{1/2}\sim 90$ s. The recoil during the decay into ^{57}Fe creates Fe_i and a vacancy, separated by an estimated 5–10 Å.

In addition to an unknown Fe center, three defects have been identified. At lower temperatures, interstitial iron Fe_i (recoil speed $d=0.76-0.86$ mm/s) dominates. Annealing increases the fraction of a center labeled Fe_N with $d=0.44-0.51$ mm/s. The concentration of this photosensitive center reaches a maximum at about 600–750 K and is interpreted as a $\{FeV\}$ pair. Its formation[17] involves an activation energy for diffusion of the order of 0.67–0.88 eV, consistent with the diffusion of Fe_i. At higher temperatures, substitutional iron Fe_s dominates, with a much smaller recoil speed $d=-0.08$ to $+0.03$ mm/s. Its occurrence correlates with high vacancy concentrations. Dynamics at 600 K suggest[18–20] that Fe_i jumps into vacancies. However, no defect resembling Fe_s has been reported in the EPR experiments in irradiated samples.

Further evidence for the existence of Fe_s is provided by channeling data.[21] The samples are implanted with ^{59}Mn which decays in 4.5 s into ^{59}Fe, releasing some 200 eV. The half-life of ^{59}Fe is about 45 days. Its β^- decay allows channeling pattern to be measured along various crystalline directions and then fit to various assumed sites for Fe. The channeling patterns indicate an ideal substitutional site (above 800 °C), a "displaced substitutional" site (~0.4–0.7 Å away from the substitutional site), a "displaced T" site (~0.3–0.8 Å away from the T site), as well as an unidentified random site.

Deep-level transient spectroscopy (DLTS) studies[22] in irradiated and Fe-contaminated samples show that anomalous early stages (~150 °C) of annealing of divacancies correlate with the appearance of a new donor level at $E_v+0.184$ eV, attributed to a Fe-divacancy complex. This defect is stable up to at least 400 °C, the maximum annealing temperature used in these experiments.

Kustov *et al.*[23] investigated the formation of Fe complexes in e^--irradiated samples with different C concentrations. They reported that, following irradiation, the concentration $[Fe_i]$ of interstitial iron drops to 1/3 of its initial value if $[C]=5\times10^{16}$ cm^{-3} and to 2/3 of its initial value if $[C]=4\times10^{17}$ cm^{-3}. However, no evidence for direct Fe-C interactions was given. Indeed, substitutional C is a major trap for self-interstitials in irradiated material,[7] resulting in an excess vacancies as well as interstitial C defects. The drop in $[Fe_i]$ could result from for example from Fe_i-V or Fe_i–C_i interactions.

It has been reported[24] that Fe prevents the precipitation of O_i, but also that it enhances it.[25–27] There is evidence that Fe enhances the formation of O-induced stacking faults.[28–30] These correlations do not necessarily imply the existence of Fe-O complexes since Si_i's are generated by oxygen precipitation. Electrical studies[31] of a deep hole trap, the T_3 center in Cz-Si, show that it consists of two defects. T_{3a} occurs only in as-grown Cz-Si and is identified with residual Fe_i impurities. T_{3b}, with a level at $E_v+0.33$ eV, occurs only in thermally treated and slow-cooled samples. It is proposed to be a complex involving Fe and several O impurities.

Several authors[32,33] have reported that, in irradiated samples, a new acceptor level at $E_c-0.36$ eV appears following ~100 °C annealings. The intensity of this DLTS signal correlates[22,34,35] with the disappearance of the A center, which normally anneals out around 350 °C. This effect only appears in samples containing Fe, and the formation of a $\{FeOV\}$ complex was proposed.

Kustov *et al.*[23] also reported a decrease in the concentration of A centers during iron precipitation. Wünstel and Wagner[36] reported the appearance of a level at $E_v+0.33$ eV after slow cool following Fe in-diffusion, and assigned it to an iron-oxygen complex. This level is also observed[31] in the slow-cooled samples of Castaldini *et al.* but was interpreted in terms of a $\{FeO_n\}$ complex. Mchedlidze and Matsumoto[37] observed by electrically detected magnetic resonance (EDMR), a new signal which correlates with the Fe concentration and is seen in O_i-rich Cz-Si but not in FZ-Si. The trigonal EDMR signal detected after Fe contamination converts to orthorhombic symmetry following long annealings at 450 °C, the temperature at which O-related thermal donors form.

Thus, a large number of Fe-related defects are seen in irradiated, implanted, and/or annealed Si samples. However, the experimental information and/or the tentative identifica-

tion provided by various authors is sometimes inconsistent or even contradictory. Few if any of these defect centers are satisfactorily identified. Our goal is to predict which types of defects occur when iron is allowed to interact with preexisting native defects, which we assume to be provided by some energetic process.

III. METHODOLOGY

The details of our approach are detailed in the first[3] of this series of papers on Fe in Si. Therefore, we restrict ourselves here to a brief overview. The host crystal is represented by periodic supercells. The nuclear dynamics are carried out using *ab initio* molecular-dynamics (MD) simulations. The core regions are removed from the calculations with *ab initio* type pseudopotentials and the electronic problem is solved within first-principles spin-density-functional theory.[38]

The calculations are carried out using two packages, VASP (Refs. 39–42) and SIESTA,[43,44] within the generalized gradient approximation for the exchange-correlation potential (see Ref. 45 for VASP and Ref. 46 for SIESTA). As shown in Ref. 3, the results predicted by the two methods are very close to each other. The results presented here are mostly obtained using SIESTA, but VASP has been used to double-check some results. These situations are indicated in the paper.

The VASP calculations use ultrasoft Vanderbilt-type pseudopotentials[47] which are included in the VASP package, and plane-wave basis sets with a cutoff of 321 eV. The SIESTA calculations use norm-conserving pseudopotentials in the Troullier–Martins form.[48] The basis sets for the valence regions are linear combinations of numerical atomic orbitals.[43,49,50] We use double-zeta basis sets (two sets of valence s and p's) for B, C, and O, and double-zeta polarized basis sets (two sets of valence s and p's plus one set of d's) for Si and Fe. The charge density is projected on a real-space grid with an equivalent cutoff of 250 Ry to calculate the exchange-correlation and Hartree potentials.

The SIESTA Fe pseudopotential has been optimized by Izquierdo *et al.*[51] and García-Suárez *et al.*[52] It includes nonlinear core corrections. We use the same orbital populations in VASP as in SIESTA. The SIESTA pseudopotential for other elements have been optimized using the experimental bulk properties of the perfect solids and/or first-principles calculations[53] as well as vibrational properties of free molecules or known defects, when experimental data are available. This testing leads to some fine tuning of the pseudopotential parameters relative to the purely atomic ones: small changes in the core radius and/or orbital populations. Once optimized, we take these pseudopotentials to be transferable to the defect problems at hand. Note that Pruneda *et al.*[54] have studied Fe/Si systems and shown that the pseudopotential/SIESTA approach provides results in excellent agreement with the all-electron tight-binding linear muffin-tin orbital method.

The host crystal is represented by a 64 host atoms periodic supercell. The lattice constant of the perfect cell is optimized. The defect geometries are optimized with a conjugate gradient algorithm. A $2\times2\times2$ Monkhorst–Pack[55] mesh is used to sample the Brillouin zone except for the calculation of dynamical matrices and gap levels.

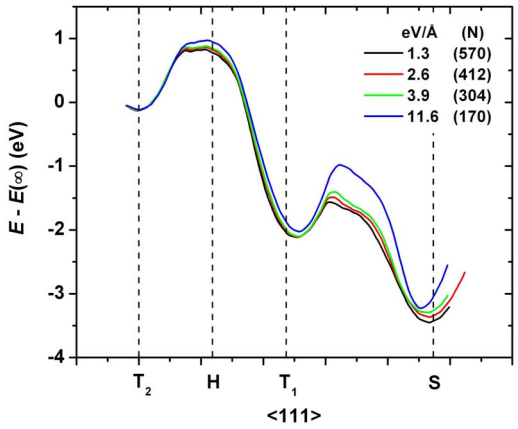

FIG. 1. (Color online) Energetics of Fe_i forced to move at constant speed along the ⟨111⟩ direction from a T site (T_2) over the hexagonal site (H) to the T site (T_1) nearest to the vacancy, then into the vacancy past the substitutional site (S). The constant force (eV/Å) used and the number (N) of time steps along the trajectory are indicated. A large force (small N) means that the crystal has little time to relax as Fe moves. The zero of the energy $E(\infty)$ corresponds to Fe_i infinitely far away from the vacancy. Qualitatively similar curves are obtained in various charge and spin states.

The dynamical matrices are calculated using the force-constant method with k-point sampling restricted to the Γ point. The gap levels are estimated using the marker method.[56] We choose the perfect crystal as a reference point since no single marker is appropriate for all the defects studied in the paper. Our best estimates for the gap levels are obtained with a $3\times3\times3$ k-point sampling. Reference 3 contains a compilation of measured and calculated (with the same approach) donor and acceptor levels for various Fe-related defects in Si. The average error for both acceptor and donor levels is 0.06 eV, with a maximum of 0.14 eV.

IV. Fe_i AND A PREEXISTING V

We performed a series of MD simulations in which the Si atoms in the supercell are allowed to relax but the Fe atom is forced to move at constant speed along a trigonal axis starting near a T site, over the hexagonal site to the T site nearest to the vacancy, then into the vacancy. In order to achieve a constant speed, we reset the velocity of the Fe to zero at each time step. Such a "quasistatic" calculation of the potential energy surface allows us to evaluate the importance of the relaxation of the host crystal. Indeed, if we push Fe very slowly, the crystal has plenty of time to relax for each intermediate position of the impurity and we obtain an adiabatic potential energy surface. If instead we push Fe very fast, the crystal has little time to relax at all, a situation similar to the frozen-crystal approximation. Figure 1 shows that the interactions between (neutral) Fe_i and a preexisting (neutral) vacancy lead to two distinct defects; the trigonal (C_{3v}) iron-vacancy pair $\{Fe_iV\}$ and the tetrahedral substitutional iron Fe_s. The two defects are compared in Fig. 2.

A. $\{Fe_iV\}$

The barrier that Fe_i must overcome to hop from the $\{Fe_iV\}$ configuration to the substitutional site and become Fe_s varies

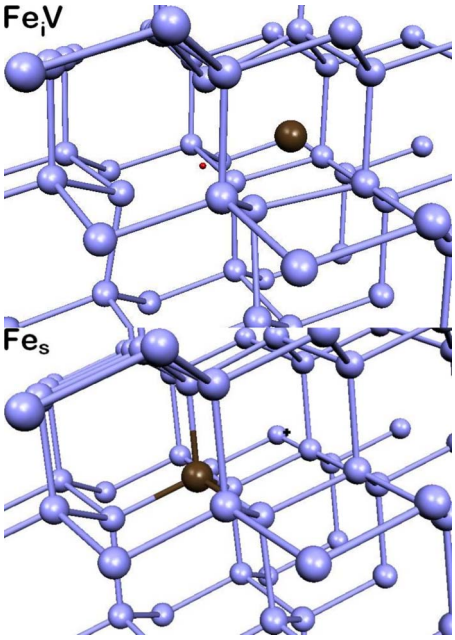

FIG. 2. (Color online) The $\{Fe_iV\}$ pair (top) has Fe_i trapped outside V on a trigonal axis. The tetrahedral Fe_s (bottom) is on site at an almost unrelaxed substitutional site. The location of the perfect T and S sites are marked by a cross and a small circle, respectively.

from 0.45 to 0.75 eV, depending on the amount of lattice relaxation allowed, the spin, and charge state. The height of this barrier is consistent with the thermal stability (160 °C) of the NL19 EPR center.[9] The stable spin states are $^{1/2}\{Fe_iV\}^-$ ($^{3/2}\{Fe_iV\}^-$ is 0.21 eV higher in energy) and $^1\{Fe_iV\}^0$ ($^0\{Fe_iV\}^0$ and $^2\{Fe_iV\}^0$ are 0.06 and 0.35 eV higher in energy), while $^{1/2}\{Fe_iV\}^+$ and $^{3/2}\{Fe_iV\}^+$ are nearly degenerate (within 0.04 eV). Note that an electron in a valence orbital overlaps with other electrons in the system and its spin easily flips to the ground state configuration. In contrast, a localized spin, such as a nuclear spin, remains very stable unless a magnetic field is present. The binding energies of $^1\{Fe_iV\}^0$ and $^{1/2}\{Fe_iV\}^+$ relative to isolated $^1Fe_i^0$ and $^{3/2}Fe_i^+$ plus an isolated vacancy are 1.62 and 1.50 eV, respectively.

The iron atom is located 0.23, 0.18, and 0.20 Å away from the ideal T site in the −, 0, and + charge states, respectively. The equilibrium site of iron in $\{Fe_iV\}$ makes this defect a possible candidate as the "off-T-site" species observed in channeling experiments.[21]

The $\{Fe_iV\}$ pair has a donor and an acceptor level in the gap, which we calculate to be at $E_v+0.35$ eV and $E_c-0.71$ eV, respectively. For comparison, isolated Fe_i has only a donor level[3] at $E_v+0.37$ eV (measured[2] $E_v+0.39-0.45$ eV).

B. Fe_s

Fe_s is stable at the ideal substitutional site with T_d symmetry. The energy difference between $^0Fe_s^0$ and isolated $^0V^0$ and $^1Fe_i^0$ is 2.92 eV. This binding energy is substantial, but smaller than the formation energy of the vacancy which is on the order of 3.4–4.0 eV.[57] Thus, while unable to create a vacancy to become substitutional, Fe_i readily interacts with a preexisting one.

In agreement with earlier theoretical predictions based on Green's functions calculations,[58,59] we find no donor level associated with Fe_s. Thus, the donor level of Fe_i is passivated by the vacancy. We also agree with the Green's functions predictions that, in the neutral charge state, the spin state of Fe_s is 0, making it invisible to EPR ($^1Fe_s^0$ is higher in energy by 0.32 eV). This low value of the spin reflects the fact that the d orbitals of Fe hybridize with the reconstructed bonds of the neutral vacancy, resulting in electron pairing in covalent bonds.

In contrast to the earlier predictions,[58,59] we find a deep acceptor level at $E_C-0.41$ eV (VASP: $E_C-0.29$ eV). In n-type material, substitutional iron is $^{1/2}Fe_s^-$. Note that Kaminski *et al.*[15] conclude their study with the following: "…we can tentatively assign the trap P11 (380 meV) to an acceptor state of Fe_s." While short of a proof, this statement combined with our results suggest that further experimental studies of this center are desirable.

V. $\{Fe_iB_s\}$ PAIR AND A PREEXISTING V

Since vacancies are mobile at room temperature and the $\{Fe_iB_s\}$ pair is common in Fe-contaminated p-type Si, we considered the possibility that these two defects interact. The most stable complex is trigonal with Fe_s and B_s at adjacent substitutional sites,

$$^{3/2}\{Fe_iB_s\}^0 + {}^0V^0 \rightarrow {}^{3/2}\{Fe_sB_s\}^0 + 2.38 \text{ eV}.$$

Another 0.32 eV is gained by reaching the ground state $^{1/2}\{Fe_sB_s\}^0$. Here again, the gain in energy is too small for this reaction to occur spontaneously. The vacancy must be provided.

The $\{Fe_sB_s\}$ defect has no donor level but a deep acceptor level at $E_c-0.84$ V. For comparison, the $\{Fe_iB_s\}$ pair has a donor and an acceptor level[3] at $E_v+0.11$ eV and $E_c-0.29$ eV, respectively (the calculated and measured values coincide for this defect). As was the case for Fe_s, the vacancy passivates the donor level of $\{Fe_iB_s\}$ when forming $\{Fe_sB_s\}$.

VI. Fe_i AND A PREEXISTING V_2

As in the case of Fe_i+V, we performed a series of MD simulations in which the Si atoms in the supercell are allowed to relax, while the Fe atom is forced to move at constant speed along the trigonal axis starting near a T site, over the hexagonal site to the T site nearest to V_2 then into the divacancy. Figure 3 shows that the interactions between (neutral) Fe_i and a preexisting (neutral) divacancy lead to two trigonal defect centers: the $\{Fe_iV_2\}$ (C_{3v}) and $\{VFeV\}$ (D_{3d}) complexes. The two defects are compared in Fig. 4.

A. $\{Fe_iV_2\}$

The barrier that Fe must overcome from $\{Fe_iV_2\}$ to hop into the divacancy, 0.8–1.5 eV, depending on the amount of relaxation allowed and the spin and/or charge states, is much

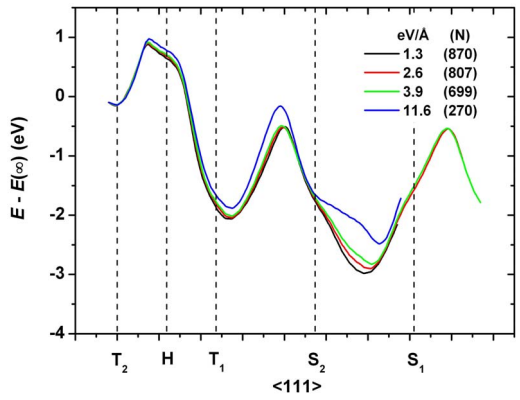

FIG. 3. (Color online) Energetics of Fe_i forced to move at constant speed along the ⟨111⟩ direction from a T site (T_2) over the hexagonal site (H) to the T site (T_1) nearest to V_2, then into the divacancy through the two substitutional sites (S_2 and S_1, respectively). The constant force used (eV/Å) and the number (N) of time steps needed to cover the trajectory for the various runs are indicated in the figure. A large force (small N) means that the crystal has little time to relax as Fe moves. The zero of the energy $E(\infty)$ corresponds to Fe_i infinitely far away from the divacancy. Qualitatively similar curves are obtained in various charge and spin states.

higher than in the case of Fe hopping from $\{Fe_iV\}$ into V. One reason for the higher barrier is that V_2 reconstructs differently from V. Another reason is that, in the lowest-energy configuration, Fe is not at the nearest substitutional site but farther away, halfway between the two vacancies. The high barrier implies that $\{Fe_iV_2\}$ is stable up to considerably higher temperatures than $\{Fe_iV\}$. However, the immediate environment around the Fe atom is similar for both trigonal $\{Fe_iV\}$ and $\{Fe_iV_2\}$ defects. The small differences in the g factors between NL19 and TU2 could result from small differences in the host crystal relaxations around $\{Fe_iV\}$ vs $\{Fe_iV_2\}$ rather than to some misalignment of the sample[14] or to the existence of two centers.

The stable spin states are $^{1/2}\{Fe_iV_2\}^-$ ($^{3/2}\{Fe_iV_2\}^-$ is 0.15 eV higher in energy), $^{1}\{Fe_iV_2\}^0$ ($^{0}\{Fe_iV_2\}^0$ and $^{2}\{Fe_iV_2\}^0$ are 0.19 and 0.21 eV higher in energy), while $^{3/2}\{Fe_iV_2\}^+$ and $^{1/2}\{Fe_iV_2\}^+$ are degenerate (within 0.01 eV). Thus, while $^{3/2}\{Fe_iV_2\}^+$ is not consistent with any of the NL defects,[9] it is consistent with the TU center observed by Mchedlidze and Suezawa.[11–13] Since the samples in the latter experiments have been subject to 3 MeV e^- irradiation (in contrast to 1.8 MeV in Ref. 9), higher concentrations of divacancies could be present. An additional complication in the EPR spectrum could result from the coexistence of $^{3/2}\{Fe_iV_2\}^+$ and $^{1/2}\{Fe_iV_2\}^+$.

The binding energies of $\{Fe_iV_2\}$ in the 0 or + charge states relative to isolated $^0V_2^0$ and $^1Fe_s^0$ or $^{3/2}Fe_s^+$ are 1.69 and 1.57 eV, respectively. The iron atom is 0.51, 0.50, and 0.35 Å away from the ideal T site in the −, 0, and + charge states, respectively. As was the case for $\{Fe_iV\}$, the equilibrium site of iron in $\{Fe_iV_2\}$ makes this defect a possible candidate to be the off-T-site species observed in channeling experiments.[21]

The $\{Fe_iV_2\}$ complex has a donor and an acceptor level in the gap, which we calculate to be at $E_v+0.25$ eV and $E_c-0.75$ eV, respectively. The position of the donor level is consistent with the DLTS center at $E_v+0.184$ eV reported by Komarov.[22] The appearance of this center correlates with the disappearance of divacancies. It is stable up to at least 400 °C.

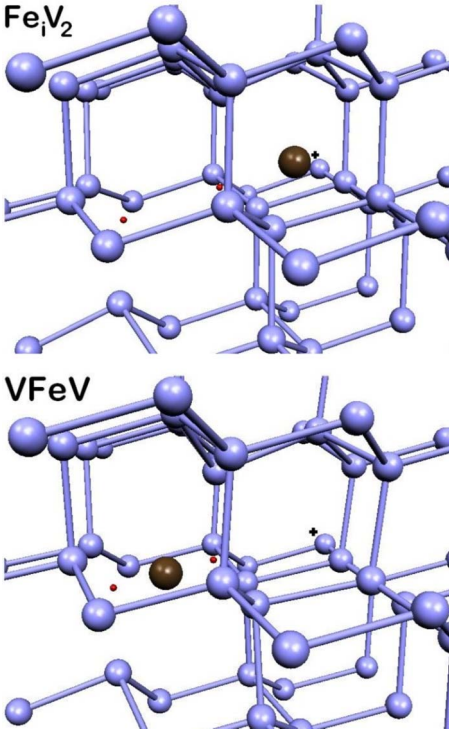

FIG. 4. (Color online) The $\{Fe_iV_2\}$ pair (top) has Fe_i trapped outside V_2 on a trigonal axis. The trigonal $\{FeVFe\}$ defect (bottom) has Fe halfway between the two vacancies. The locations of the perfect T and S sites are marked by a cross and small circles, respectively.

B. {VFeV}

The iron-divacancy defect $\{VFeV\}$ has a sixfold Fe located halfway between the two vacancies. In the − charge state, the $^{1/2}\{VFeV\}^-$ and $^{3/2}\{VFeV\}^-$ are degenerate (within 0.02 eV). In the 0 charge state, the stable spin state is $^{1}\{VFeVF\}^0$ ($^{0}\{VFeV\}^0$ and $^{2}\{VFeV\}^0$ are 0.56 and 0.15 eV higher in energy). $\{VFeV\}$ has no donor level.

If isolated $^1Fe_i^0$ traps at a preexisting divacancy and forms $^{1}\{VFeV\}^0$, the gain is energy is 3.02 eV. If $^0V^0$ traps at $^{1}\{Fe_iV\}^0$ and forms $^{1}\{VFeV\}^0$, the gain in energy is 2.86 eV. Finally, if $^0Fe_s^0$ traps a vacancy and forms $^{1}\{VFeV\}^0$, the gain in energy is 1.56 eV.

The perfect crystal is a good marker for donor levels, and often works well for single acceptor levels, but it is not a good marker for double acceptor levels. The single and double acceptor levels of the isolated divacancy are known[60] to be at $E_c-0.42$ eV and $E_c-0.23$ eV, respectively. Therefore, we used the isolated divacancy as a marker in the case of $\{VFeV\}$. We then find that $\{VFeV\}$ has a single and a double acceptor levels at $E_c-0.73$ eV (VASP: $E_c-0.64$) and $E_c-0.55$ eV (VASP: $E_c-0.48$), respectively.

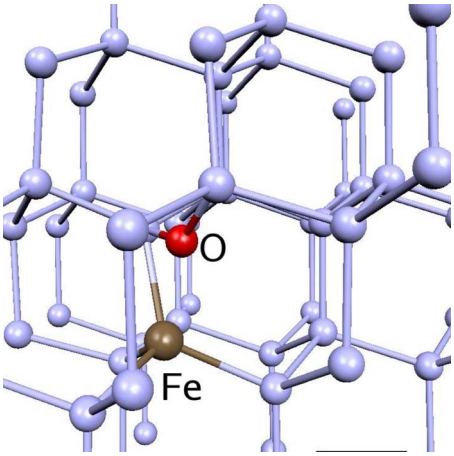

FIG. 5. (Color online) If Fe_i encounters the A center, it pushes O out of the vacancy and takes its place. The $\{Fe_sO_i\}$ defect has interstitial oxygen bridging one of the Si-Si bonds adjacent to Fe_s.

VII. Fe_i AND THE A CENTER

An immediate consequence of the irradiation of Cz-Si is the trapping of a vacancy by O_i resulting in the $\{OV\}$ defect, better known as the A center.[4,5] We performed constant-temperature MD simulations in the range of 800–1000 K with a 1.0 fs time step, starting with Fe_i at a T site nearest to $\{OV\}$. After a few thousand time steps, Fe had pushed O out of the vacancy and become substitutional, while O bridges one of the nearest Si-Si bonds (Fig. 5), forming the $\{Fe_sO_i\}$ defect. The reaction occurs at a substantial gain in energy,

$$^1Fe_i^0 + {}^0\{OV\}^0 \rightarrow {}^1\{Fe_sO_i\}^0 + 1.91 \text{ eV}.$$

Another 0.1 eV energy gain occurs when a spin flips to the stable $^0\{Fe_sO_i\}^0$ configuration. This configuration is more stable than isolated O_i and $^0Fe_s^0$ by 0.3 eV. Note that interstitial copper encountering the A center has been predicted[62] to exhibit similar behavior, except that the lowest-energy configuration is not a $\{Cu_sO_i\}$ defect but isolated O_i and $Cu_s:Cu_i+\{OV\} \rightarrow Cu_s+O_i+2.13$ eV.

The $\{Fe_sO_i\}$ defect has no donor level but an acceptor level at $E_c-0.36$ eV. In n-type material, the stable state is $^{1/2}\{Fe_sO_i\}^-$ (the $^{3/2}\{Fe_sO_i\}^-$ state is 0.22 eV higher in energy). This calculated acceptor level coincides with that associated by several authors[22,34,35] with an unidentified $\{FeOV\}$ complex, the formation of which correlates with the disappearance of the A center.

The asymmetric stretch of O in $^0\{Fe_sO_i\}^0$ is at 1065 cm^{-1}. For comparison, the calculated (measured[61]) local vibrational modes (LVMs) of O_i and the A center are at 1144 cm^{-1} (1136 cm^{-1}) and 809 cm^{-1} (836 cm^{-1}), respectively.

VIII. Fe_i AND A PREEXISTING Si_i

The possibility of interactions between Fe_i and a self-interstitial has not been considered in the interpretation of the experimental data since most of the samples used in the e^--irradiation studies were FZ-Si, in which the dominant impurity is C_s, a well-known trap for self-interstitial, resulting in the formation of C_i and related complexes.[63] These samples tend to be vacancy-rich following irradiation. However, some concentration of Si_i remains present. Further, the dominant impurity in Cz-Si is O_i, a strong trap for vacancies (resulting in the formation of A centers). Therefore, e^--irradiated Cz-Si tends to be rich in self-interstitials.

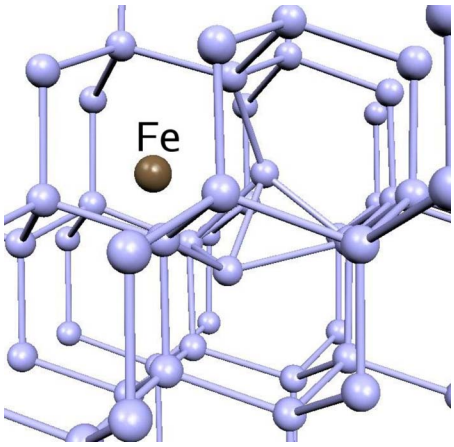

FIG. 6. (Color online) If Fe_i encounters a preexisting self-interstitial, it forms the $\{Fe_iSi_i\}$ defect with a gain in energy of over 1 eV.

The interactions between Fe_i and Si_i are not as energetic as those involving vacancies, but trapping occurs nonetheless. Figure 6 shows the lowest-energy configuration of the $\{Fe_iSi_i\}$ pair. The Fe_i-Si_i direction is slightly off a 110 axis, while isolated Si_i is exactly along on that axis.[64] The pair has a donor level at $E_v+0.42$ eV, quite close to that of isolated Fe_i, and no acceptor level.

The stable spin states are $^1\{Fe_iSi_i\}^0$ ($^0\{Fe_iSi_i\}^0$ is very close, 0.05 eV higher in energy) and $^{3/2}\{Fe_iSi_i\}^+$ is ($^{1/2}\{Fe_iSi_i\}^+$ 0.08 eV higher in energy). The binding energy relative to the isolated $^{3/2}Fe_i^+$ and $^0Si_i^0$ is 1.07 eV, and the $\{Fe_iSi_i\}$ complex is stable well above room temperature. Thus, Fe_i could play a role in facilitating the precipitation of oxygen by providing a low-energy trap for the self-interstitials that are generated during this process. Further, Fe_i is likely to trap at self-interstitial clusters and/or dislocation loops near O precipitates.

IX. Fe_i AND C_i

An immediate consequence of the irradiation of FZ-Si is the trapping of a self-interstitial by C_s resulting in the formation of C_i.[6,7] We optimized the geometries of all the possible configurations involving Fe_i and C_i. The binding energies relative to isolated C_i and Fe_i are rather small

$$^1Fe_i^0 + {}^0C_i^0 \rightarrow {}^1\{Fe_iC_i\}^0 + 0.52 \text{ eV}$$

and

$$^{3/2}Fe_i^+ + {}^0C_i^0 \rightarrow {}^{3/2}\{Fe_iC_i\}^+ + 0.73 \text{ eV}.$$

The donor and acceptor levels of the $\{Fe_iC_i\}$ pair are at $E_v+0.67$ eV and $E_c-0.44$ eV, respectively. The stable spin states are $^{3/2}\{Fe_iC_i\}^-$ (the $^{1/2}\{Fe_iC_i\}^-$ state is 0.11 eV higher

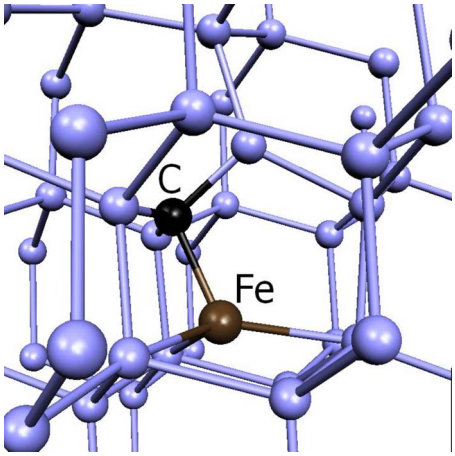

FIG. 7. (Color online) When Fe_i encounters a carbon interstitial, it forms the $\{Fe_iC_i\}$ pair with a maximum gain in energy of about 0.7 eV (+ charge state).

in energy), $^{1}\{Fe_iC_i\}^0$ (the $^{0}\{Fe_iC_i\}^0$ and $^{2}\{Fe_iC_i\}^0$ states are 0.42 and 0.11 eV higher in energy, respectively), and $^{3/2}\{Fe_iC_i\}^+$ (the $^{1/2}\{Fe_iC_i\}^-$ state is 0.16 eV higher in energy). The structure is nearly identical in all three charge states (Fig. 7).

The LVMs of C_i in $^{3/2}\{Fe_iC_i\}^-$ are at 848 and 746 cm^{-1}. For comparison, the calculated[65] LVMs of isolated C_i are at 969 and 903 cm^{-1} (measured:[66] 931 and 920 cm^{-1}), respectively.

X. Fe_i AND C_s, O_i, $\{O_iO_i\}$

Interstitial oxygen and substitutional carbon are the most common impurities in Cz-Si and FZ-Si, respectively. Even though there is no direct evidence[2] of complexes involving Fe_i and either O_i or C_s, we considered the possibility of interactions between these species.

We find no $\{Fe_iC_s\}$ complex in the + or 0 charge states (the most stable configurations is 0.07 or 0.24 eV less stable than the isolated species, respectively). This result is not very surprising since typical Si-C and Fe-C bond strengths[67] are 4.5 and 1.6 eV, respectively, implying that C will always prefer to bind to Si rather than Fe.

Similarly, there are no stable configurations with Fe_i at or near any T site adjacent to O_i. The most stable structure is 0.02 eV less stable than the isolated impurities. As for Fe_i near the $\{O_iO_i\}$ pair, the binding energy in the + charge state (spin 3/2) is a tiny 0.04 eV, a number far too small to compensate for nonzero temperature effects.[68] Thus, we find that no interactions take place between Fe_i and either O_i or the $\{O_iO_i\}$ pair. Here again, typical bond strengths[67] strongly favor Si-O (8.0 eV) over Fe-O (3.9 eV) bonding.

XI. DISCUSSION

First-principles theory is used to predict the interactions between Fe_i and a range of defects resulting from energetic processes such as implantation or irradiation: V, V_2, $\{OV\}$, Si_i, and C_i. In the case of the monovacancy, interactions with both Fe_i and the $\{Fe_iB_s\}$ pair are considered. For completeness, we also study the interactions between Fe_i and the most common impurities in as-grown FZ- and Cz-Si, C_s, and O_i, respectively, as well as the $\{O_iO_i\}$ dimer. The configurations, charge and spin states, binding energies, and approximate acceptor and donor levels of $\{Fe_iV\}$, Fe_s, $\{Fe_sB_s\}$, $\{Fe_iV_2\}$, $\{VFeV\}$, $\{Fe_sO_i\}$, $\{Fe_iSi_i\}$, and $\{Fe_iC_i\}$ are predicted. To facilitate experimental identification, we also calculate the LVMs associated with $\{Fe_sO_i\}$ and $\{Fe_iC_i\}$. There is no binding energy between Fe_i and C_s, O_i, or $\{O_iO_i\}$.

A. Common features and trends

The strongest interactions involve Fe_i and vacancylike defects. In the four cases investigated here (vacancy, iron-boron pair, divacancy, and A center), the most stable complex has Fe inside the void, covalently bound to the host crystal, with a gain in energies of 2.0 eV ($\{Fe_sO_i\}$), 2.7 eV ($\{Fe_sB_s\}$), 2.9 eV (Fe_s), and 3.0 eV ($\{VFeV\}$), relative to isolated Fe_i and $\{OV\}$, V and $\{Fe_iB_s\}$, V and Fe_i, and V_2 and Fe_i, respectively.

In the case of Fe_i interacting with V or V_2, a metastable defect is generated, $\{Fe_iV\}$ or $\{Fe_iV_2\}$, respectively. It involves Fe_i trapped off the T site, along the trigonal axis, but outside V or V_2. The binding energy relative to isolated Fe_i is of the order of 2 eV and the barrier that Fe_i must overcome to reach the stable configuration (Fe_s and $\{VFeV\}$, respectively) is of the order of 0.6 and 1.2 eV, respectively. The precise values of these energies depend on the charge and spin state.

Upon formation of $\{Fe_sB_s\}$, $\{Fe_sO_i\}$, Fe_s, and $\{VFeV\}$, the donor level associated with interstitial iron ($\sim E_v+0.4$ eV) disappears and an acceptor level appears at $E_c-0.84$ eV, $E_c-0.36$ eV, $E_c-0.41$ eV, and $E_c-0.73$ eV, respectively. The passivation by vacancies of the donor levels of both Fe_i and $\{Fe_iB_s\}$ has consequences. For example, an injection of vacancies occurs during the high-temperature annealing that follows the deposition of an SiN_x antireflection coating on Si solar cells.[69] This treatment generally improves the efficiency of cells, as H diffuses from the surface layer into the bulk which results in the passivation of some defect centers. Our results show that vacancy injection could also play a role in this process by passivating the deep donor activity of Fe_i and $\{Fe_iB_s\}$.

All the complexes which contain interstitial iron, namely, $\{Fe_iV\}$, $\{Fe_iV_2\}$, $\{Fe_iSi_i\}$, and $\{Fe_iC_i\}$, have a donor level in the gap at $E_v+0.35$ eV, $E_v+0.25$ eV, $E_v+0.42$ eV, and $E_v+0.67$ eV, respectively. These levels are close to that of isolated Fe_i (calculated[3] $E_v+0.37$ eV and measured[2] $E_v+0.39-0.45$ eV).

The complexes which involve Fe_i and either C_i or a vacancy, namely, $\{Fe_iC_i\}$, $\{Fe_iV\}$, and $\{Fe_iV_2\}$, also have a deep acceptor level in the gap, $E_c-0.44$ eV, $E_c-0.71$ eV, and $E_c-0.75$ eV, respectively. In the case of $\{VFeV\}$, a double acceptor level at $E_c-0.55$ eV is present. Figure 8 shows the calculated gap levels associated with all the defects considered here, compared to isolated Fe_i and the $\{Fe_iB_s\}$ pair.

When Fe_i interacts with the A center, it expels O from the vacancy, and takes its place, with a 2 eV gain of energy. The

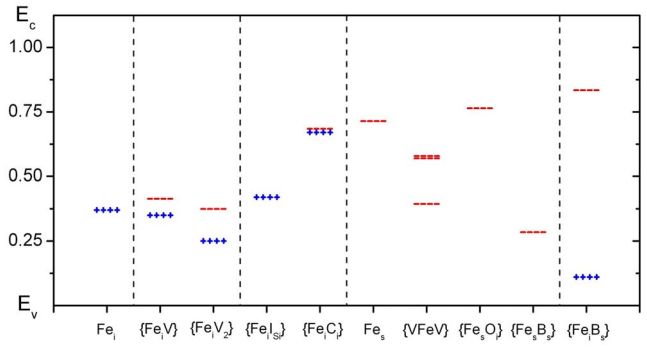

FIG. 8. (Color online) Calculate donor (+ signs, blue) and acceptor (minus signs, red) levels associated with various Fe-related defects. The double acceptor level of {*V*Fe*V*} is marked with =signs (red). The calculated gap levels of Fe_i and $\{Fe_iB_s\}$ match the experimental values[3] and the calculated donor level of Fe_s is close to the P11 trap reported by Kaminski *et al.* (Ref. 15).

result is the $\{Fe_sO_i\}$ defect. The O-related LVM in $^0\{Fe_sO_i\}^0$ is at 1065 cm^{-1}. Fe_i also traps at C_i. The binding energy of this pair is smaller, at best 0.7 eV in the case of $^{3/2}\{Fe_iC_i\}^+$. The C-related LVMs are at 848 and 746 cm^{-1}.

B. Connection to observed defects

The calculated properties of $^{3/2}\{Fe_iV\}^+$ and $^{3/2}\{Fe_iV_2\}^+$ are consistent with those of the NL19 and TU2 EPR centers, respectively. Either one of these two defects could be the off-*T*-site center(s) observed in the Mössbauer and channeling experiments since the only experimental signature in this case is an approximate location of the Fe atom.

The closest defect we find that could be identified with the off-substitutional site reported in the channeling data is {*V*Fe*V*}. However, in this defect, Fe is about 1.2 Å away from a perfect substitutional site, about twice the experiment value (0.4–0.7 Å). Further, there is no evidence that high concentrations of V_2 are generated in the channeling experiments. In the $\{Fe_sO_i\}$ defect, Fe is almost exactly at the substitutional site. The off-substitutional site reported in the channeling experiments remains unidentified.

$\{Fe_sO_i\}$, characterized by a level at $E_c-0.36$ eV, is likely to be the {Fe*V*O} center reported in DLTS studies.[22,34,35] The formation of the defect occurs at a temperature where Fe_i is highly mobile, the large binding energy is consistent with the high annealing temperatures reported, and the gap level is just right.

ACKNOWLEDGMENTS

This work of SKE is supported in part by the National Renewable Energy Laboratory, the Silicon Solar Consortium, and the grant D-1126 from the R. A. Welch Foundation. The work of MS is supported by a grant from the Advanced Research Program of the State of Texas. Many thanks to Texas Tech's High Performance Computer Center for generous amounts of computer time.

*stefan.estreicher@ttu.edu

[1] A. A. Istratov, H. Hieslmair, and E. R. Weber, Appl. Phys. A: Mater. Sci. Process. **70**, 489 (2000).
[2] A. A. Istratov, H. Hieslmair, and E. R. Weber, Appl. Phys. A: Mater. Sci. Process. **69**, 13 (1999).
[3] M. Sanati, N. G. Szwacki, and S. K. Estreicher, Phys. Rev. B **76**, 125204 (2007).
[4] G. W. Watkins and J. W. Corbett, Phys. Rev. **121**, 1001 (1961); J. W. Corbett, G. D. Watkins, R. M. Chrenko, and R. S. McDonald, *ibid.* **121**, 1015 (1961).
[5] B. Pajot, in *Oxygen in Silicon*, edited by F. Shimura (Academic, Boston, 1994), p. 191.
[6] G. W. Watkins and K. L. Brower, Phys. Rev. Lett. **36**, 1329 (1976).
[7] G. Davies, A. S. Oates, R. C. Newman, R. Wooley, E. C. Lightowlers, M. J. Binns, and J. G. Wilkes, J. Phys. C **19**, 841 (1986).
[8] B.-D. Choi, D. K. Schroder, S. Koveshnikov, and S. Mahajan, Jpn. J. Appl. Phys., Part 2 **40**, L915 (2001).
[9] S. H. Muller, G. M. Tuynman, E. G. Sieverts, and C. A. J. Ammerlaan, Phys. Rev. B **25**, 25 (1982).
[10] J. J. van Kooten, E. G. Sieverts, and C. A. J. Ammerlaan, Solid State Commun. **64**, 1489 (1987).
[11] T. Mchedlidze and M. Suezawa, Physica B **308-310**, 400 (2001); **308-310** 421 (2001).
[12] T. Mchedlidze and M. Suezawa, Physica B **324**, 188 (2002).
[13] T. Mchedlidze and M. Suezawa, Jpn. J. Appl. Phys., Part 1 **41**, 7288 (2002).
[14] T. Mchedlidze (private communication).
[15] P. Kaminski, R. Kozlowski, A. Jelenski, T. Mchedlidze, and M. Suezawa, Jpn. J. Appl. Phys., Part 1 **42**, 5415 (2001).
[16] G. Weyer, S. Degroote, M. Fanciulli, V. N. Fedoseyev, G. Langouche, V. I. Mishin, A.-M. Van Bavel, A. Vantomme, and ISOLDE collaboration, Mater. Sci. Forum **258-263**, 437 (1997); G. Weyer, A. Burchard, M. Fanciulli, V. N. Fedoseyev, H. P. Gunnlaugsson, V. I. Mishin, R. Sielemann, and the ISOLDE collaboration, Physica B **273-174**, 363 (1999).
[17] H. P. Gunnlaugsson, G. Weyer, N. E. Christensen, M. Dietrich, M. Fanciulli, K. Bharuth-Ram, R. Sielemann, A. Svane, and ISOLDE collaboration, Physica B **340-342**, 532 (2003).
[18] P. Schwalbach, S. Laubach, M. Hartick, E. Kankeleit, B. Keck, M. Menningen, and R. Sielemann, Phys. Rev. Lett. **64**, 1274 (1990).
[19] Y. Yoshida, S. Ogawa, and K. Arikawa, Physica B **340-342**, 605 (2003); Y. Yoshida, Y. Kobayashi, K. Hayakawa, K. Yukihira, A. Yoshida, H. Ueno, F. Shimura, and F. Ambe, *ibid.* **376-377**, 69 (2006).
[20] Y. Yoshida, Y. Suzuki, A. Matsushita, K. Suzuki, and K. Sakata, Physica B **401-402**, 167 (2007); Y. Yoshida, Y. Kobayashi, K. Yukihira, K. Hayakawa, K. Suzuki, A. Yoshida, H. Ueno, A. Yoshimi, K. Shimada, D. Nagae, K. Asahi, and G. Langouche, *ibid.* **401-402**, 101 (2007).

[21] U. Wahl, J. G. Correia, E. Rita, J. P. Araújo, J. C. Soares, and ISOLDE collaboration, Phys. Rev. B **72**, 014115 (2005); Nucl. Instrum. Methods Phys. Res. B **253**, 167 (2006).
[22] B. A. Komarov, Fiz. Tekh. Poluprovodn. (S.-Peterburg) **38**, 1079 (2004); [Semiconductors **38**, 1041 (2004)].
[23] V. E. Kustov, Y. N. Bagrin, N. A. Tripachko, V. I. Shakhovtsov, and L. I. Spinar, Phys. Status Solidi A **129**, 337 (1992).
[24] B. Hackl, K. J. Range, L. Fabry, and P. Stallhofer, J. Electrochem. Soc. **139**, 3250 (1992).
[25] X. Zhang, D. Yang, R. Fan, J. Zhang, and D. Que, J. Appl. Phys. **84**, 5502 (1998).
[26] B. Shen, J. Jablonski, T. Sekiguchi, and K. Sumino, Jpn. J. Appl. Phys., Part 1 **35**, 4187 (1996).
[27] J. Jablonski, B. Shen, T. Mchedlidze, M. Imai, and K. Sumino, Mater. Sci. Forum **196-201**, 1859 (1995).
[28] M. Hourai, K. Murakami, T. Shigematsu, N. Fujino, and T. Shiraiwa, Jpn. J. Appl. Phys., Part 1 **28**, 2413 (1989).
[29] S. Sadamitsu, A. Sasaki M. Hourai, M. Sumita, and N. Fujino, Jpn. J. Appl. Phys., Part 1 **30**, 1591 (1991).
[30] M. Miyazaki, S. Miyazaki, T. Kitamura, T. Aoki, Y. Nakashima, M. Hourai, and T. Shigematsu, Jpn. J. Appl. Phys., Part 1 **34**, 409 (1995).
[31] A. Castaldini, D. Cavalcoli, A. Cavallini, S. Binetti, and S. Pizzini, Appl. Phys. Lett. **86**, 162109 (2005).
[32] L. C. Kimerling, Inst. Phys. Conf. Ser. **31**, 221 (1977).
[33] S. D. Brotherton and P. J. Bradley, J. Appl. Phys. **53**, 5720 (1982).
[34] C. E. Barnes, J. Electron. Mater. **8**, 437 (1979).
[35] Z. You, M. Gong, Y. Chen, and J. W. Corbett, J. Appl. Phys. **63**, 324 (1988).
[36] K. Wünstel and P. Wagner, Solid State Commun. **40**, 797 (1981).
[37] T. Mchedlidze and K. Matsumoto, J. Appl. Phys. **83**, 4042 (1998).
[38] *Theory of Defects in Semiconductors*, edited by D. A. Drabold and S. K. Estreicher (Springer, Berlin, 2007).
[39] VASP 2003 (http://cms.mpi.univie.ac.at/vasp).
[40] G. Kresse and J. Hafner, Phys. Rev. B **47**, 558 (1993).
[41] G. Kresse and J. Furthmüller, Phys. Rev. B **54**, 11169 (1996).
[42] G. Kresse and D. Joubert, Phys. Rev. B **59**, 1758 (1999).
[43] D. Sánchez-Portal, P. Ordejón, E. Artacho, and J. M. Soler, Int. J. Quantum Chem. **65**, 453 (1997).
[44] E. Artacho, D. Sánchez-Portal, P. Ordejón, A. García, and J. M. Soler, Phys. Status Solidi B **215**, 809 (1999).
[45] J. P. Perdew, *Electronic Structure of Solids '91*, edited by P. Ziesche and H. Eschring (Akademie, Berlin, 1991), p. 11.
[46] J. P. Perdew, K. Burke, and M. Ernzerhof, Phys. Rev. Lett. **77**, 3865 (1996).
[47] D. Vanderbilt, Phys. Rev. B **41**, 7892 (1990).
[48] N. Troullier and J. L. Martins, Phys. Rev. B **43**, 1993 (1991).
[49] O. F. Sankey and D. J. Niklewski, Phys. Rev. B **40**, 3979 (1989); O. F. Sankey, D. J. Niklewski, D. A. Drabold, and J. D. Dow, *ibid.* **41**, 12750 (1990).
[50] A. A. Demkov, J. Ortega, O. F. Sankey, and M. P. Grumbach, Phys. Rev. B **52**, 1618 (1995).
[51] J. Izquierdo, A. Vega, L. C. Balbás, D. Sánchez-Portal, J. Junquera, E. Artacho, J. M. Soler, and P. Ordejón, Phys. Rev. B **61**, 13639 (2000).
[52] V. M. García-Suárez, C. M. Newman, C. J. Lambert, J. M. Pruneda, and J. Ferrer, J. Phys.: Condens. Matter **16**, 5453 (2004).
[53] V. L. Moruzzi and C. B. Sommers, *Calculated Electronic Properties of Ordered Alloys: a Handbook* (World Scientific, Singapore, 1995).
[54] J. M. Pruneda, R. Robles, S. Bouarab, J. Ferrer, and A. Vega, Phys. Rev. B **65**, 024440 (2001).
[55] H. J. Monkhorst and J. D. Pack, Phys. Rev. B **13**, 5188 (1976).
[56] J. P. Goss, M. J. Shaw, and P. R. Briddon, *Theory of Defects in Semiconductors* (Ref. 38), p. 69.
[57] S. Dannefaer, P. Mascher, and D. Kerr, Phys. Rev. Lett. **56**, 2195 (1986); S. K. Estreicher, Phys. Status Solidi B **217**, 513 (2000).
[58] A. Zunger and U. Lindefelt, Phys. Rev. B **26**, 5989 (1982).
[59] F. Beeler, O. K. Andersen, and M. Scheffler, Phys. Rev. B **41**, 1603 (1990).
[60] B. G. Svensson, B. Mohadjeri, A. Hallén, J. H. Svensson, and J. W. Corbett, Phys. Rev. B **43**, 2292 (1991).
[61] B. Pajot, in *Oxygen in Silicon*, Semiconductors and Semimetals Vol. 42, edited by F. Shimura (Academic, San Diego, 1994), p. 191.
[62] D. West, S. K. Estreicher, S. Knack, and J. Weber, Phys. Rev. B **68**, 035210 (2003).
[63] R. Jones, B. J. Coomer, and P. R. Briddon, J. Phys.: Condens. Matter **16**, S2643 (2004).
[64] S. K. Estreicher, M. Gharaibeh, P. A. Fedders, and P. Ordejón, Phys. Rev. Lett. **86**, 1247 (2001).
[65] D. J. Backlund and S. K. Estreicher (unpublished).
[66] A. R. Bean and R. C. Newman, Solid State Commun. **8**, 175 (1970).
[67] *CRC Handbook of Chemistry and Physics*, 75th ed., edited by D. R. Lide (CRC, Boca Raton, FL, 1994).
[68] S. K. Estreicher, M. Sanati, D. West, and F. Ruymgaart, Phys. Rev. B **70**, 125209 (2004).
[69] S. Kleekajai, F. Jiang, M. Stavola, V. Yelundur, K. Nakayashiki, A. Rohatgi, G. Hahn, S. Seren, and J. Kalejs, J. Appl. Phys. **100**, 093517 (2006).